



Spray flames in a one-dimensional duct of varying cross-sectional area

Chih-Hsin Tsai^a, Shuhn-Shyurng Hou^{b,*}, Ta-Hui Lin^c

^a Department of Mechanical Engineering, Hsiuping Institute of Technology, Taichung, Taiwan 412, ROC

^b Department of Mechanical Engineering, Kun Shan University of Technology, 949 Da-Wan Road, Yung-Kung City, Tainan Hsien 71003, Taiwan, ROC

^c Department of Mechanical Engineering, National Cheng Kung University, Tainan, Taiwan 70101, ROC

Received 18 April 2004; received in revised form 30 December 2004

Available online 4 March 2005

Abstract

The influences of flame stretch, preferential diffusion and internal heat transfer on the extinction of dilute spray flames propagating in a duct with varying cross-sectional area are analyzed using activation energy asymptotics. A completely prevaporized mode and a partially prevaporized mode of flame are identified. The results show that the internal heat transfer, which is associated with the liquid fuel loading and the initial droplet size of the spray, provides internal heat loss for rich sprays but heat gain for lean sprays. The burning intensities of a lean (rich) spray is enhanced (further reduced) with increasing liquid fuel loading and decreasing initial droplet size. The positive stretch weakens a lean methanol-spray flame and rich ethanol-spray flame ($Le > 1$) but intensifies a rich methanol-spray flame ($Le < 1$). The flame stretch is found to dominate strongly the tendency towards flame extinction characterized by a C-shaped curve. However, for a rich methanol spray flame ($Le < 1$), an S-shaped extinction curve can be obtained if it experiences positive stretch and endures a partially prevaporized spray of a large enough fuel loading and a sufficiently large droplet size. The S-shaped curve, which differs greatly from the C-shaped one, shows that the flame extinction is governed by the internal heat loss.

© 2005 Elsevier Ltd. All rights reserved.

1. Introduction

It is well known that a homogeneous laminar premixed flame influenced by external heat loss can be described by a C-shaped extinction curve (a double-valued function) in the classical flame-quenching theory [1]. It indicates that a given combustible premixture will have two possible flame speeds under a fixed amount of

heat loss: the upper branch representing stable solution; and the lower branch showing unstable solution. The extinction limit, identified by the critical point in connecting the upper and lower branch, indicates that a sufficiently large external heat loss results in flame extinction.

Flame stretch is recognized as a very important parameter affecting flame behavior. The effects of stretch become especially prominent in the presence of preferential diffusion, i.e. when the mixture has nonunity Lewis number [2–4]. Lewis number designates the ratio of thermal-to-mass diffusivities of the deficient reactant in the

* Corresponding author. Tel.: +886 6 2050496; fax: +886 6 2050509.

E-mail address: sshou@mail.ksut.edu.tw (S.-S. Hou).

Nomenclature

Dimensional quantities

A'	cross-sectional area of duct
B'	frequency factor
C'_{PG}	specific heat of the gaseous mixture
C'_{PL}	specific heat of liquid
l'_T	preheat zone thickness, $l'_T = \lambda' / (C'_{PG} \dot{m}'_P)$
\overline{M}	average molar mass
\dot{m}'_P	flame propagation flux of a homogeneous mixture
P'	pressure
Q'_C	heat of combustion per unit mass of fuel
\tilde{R}	universal gas constant
r'	droplet radius
r'_c	critical initial droplet size

Nondimensional quantities

A_1	Eq. (7)
h_{LG}	latent heat of vaporization, h'_{LG} / Q'_C
Le	Lewis number
\dot{m}_0	flame propagation flux, \dot{m}'_0 / \dot{m}'_P
T	temperature, $T' C'_{PG} / Q'_C$
T_a	activation temperature, $E'_a C'_{PG} / (Q'_C \tilde{R})$
\tilde{W}	Eq. (8)
x	transformed coordinate, x' / l'_T
Y	$Y_F = Y'_F$ and $Y_O = Y'_O / \sigma$
Z	density ratio, ρ'_G / ρ'

Greek symbols

α	$\alpha = 1$ and $\alpha = 0$ for lean and rich flame
ε	small expansion parameter, T_∞ / T_a
γ	$Z_{-\infty} = 1 - \varepsilon \gamma$
Φ	equivalence ratio
Γ	stretch parameter

Subscripts

b	boiling state
E	state at extinction
e	state at which droplet is completely vaporized
f	flame front
F, O	fuel and oxygen
G, L	gas and liquid phases
i	$i = F$ and O in lean and rich flame
j	$j = O$ and F in lean and rich flame
v	state at which evaporation initiates
0,1	zeroth and first-order solutions
$-\infty, \infty$	initial and final states

Superscripts

+	downstream of the flame
'	dimensional quantities

mixture. For nonequidiffusive, stretched flames, the flame response exhibits opposite behavior, according to whether the stretch is positive or negative, and whether the mixture's Lewis number is greater or less than unity. For positively stretched flames in the stagnation-point flow, increasing stretch weakens/extinguishes a $Le > 1$ flame but intensifies a $Le < 1$ flame [2–4]. The converse holds for the negatively stretched Bunsen flame tip [5,6].

Additionally, the effects of area change do play a significant role in one-dimensional formulation of flame behavior [7]. There was also a study for flame propagating in a closed tube with varying cross-sectional area [8]. It was concluded that positive flame stretch increases the mass burning rate, whereas negative flame stretch has the opposite effect, for flames with a Lewis number greater (smaller) than unity.

The studies on flame extinction previously introduced were only focused on homogeneous mixture. However, the participation of fuel spray effects further produced so-called internal heat loss (or gain) to the system, and thereby resulted in an S-shaped extinction curve (a triple-valued function) on spray flame extinction [9,10].

Much attention has been paid to the burning and extinction of the dilute spray flame in a series of theoretical studies with one-dimensional models [9–11]. It was generally concluded that flame extinction characterized by a C-shaped curve is governed by external heat loss; whereas the S-shaped extinction curve is caused by the internal heat loss resulting from droplet gasification. In those studies [9–11], however, the effects of stretch and preferential diffusion on flame behavior were not examined.

The aim of this work is to analyze the influences of flame stretch, preferential diffusion and internal heat transfer on the extinction of dilute spray flames propagating in a duct with varying cross-sectional area. Here flame stretch is induced by varying cross-sectional area [7,8]. A positive flame stretch means that the flame propagates in a divergent duct, while a negative flame stretch denotes that the flame propagates in a convergent duct. The problem is analyzed using activation energy asymptotics. We shall also restrict our analysis to dilute sprays [9–11] in which the amount of liquid fuel loading in the total fresh mixture is very small and can be expanded by perturbation analysis.

2. Theoretical model

2.1. Configurations and assumptions

We adopt a one-dimensional coordinate system in which a planar flame sits at $x = 0$ in a duct with varying cross-sectional area. The two phases combustible mixture composed of various concentrations of oxidizer, nitrogen, fuel vapor, and fuel droplets of a certain radius comes from $x = -\infty$, and the equilibrium reaction products move away toward $x = +\infty$, as illustrated in Fig. 1. Fig. 1 also shows the two modes used in analysis. The modes are identified on the basis of r'_c , which is the critical initial droplet size for the droplets to achieve complete vaporization at the premixed flame front. Therefore, for the cases of $r'_{-\infty} \leq r'_c$ and $r'_{-\infty} > r'_c$ we have, respectively, the completely prevaporized mode (CPM) and the partially prevaporized mode (PPM), as shown in Fig. 1(a) and (b). We assume that the droplets will start to evaporate at $x = x_v$, where the gas temperature has reached the boiling point of the liquid. The droplets then ignite upon crossing the flame, and vanish at $x = x_e$ upon complete combustion for lean sprays or complete evaporation for rich sprays.

We assume that the spray is dilute and the amount of liquid fuel loading is of $O(\varepsilon)$ in the asymptotic analysis. Here $\varepsilon = T_\infty/T_a$ is the small parameter of expansion for large activation energy reactions in the combustion process. The motion of the droplets is in phase with that of the gas. In the evaporation process, the droplets have a constant temperature and follow the d^2 -law. Finally, we assume that the fuel and oxidizer reaction for the bulk

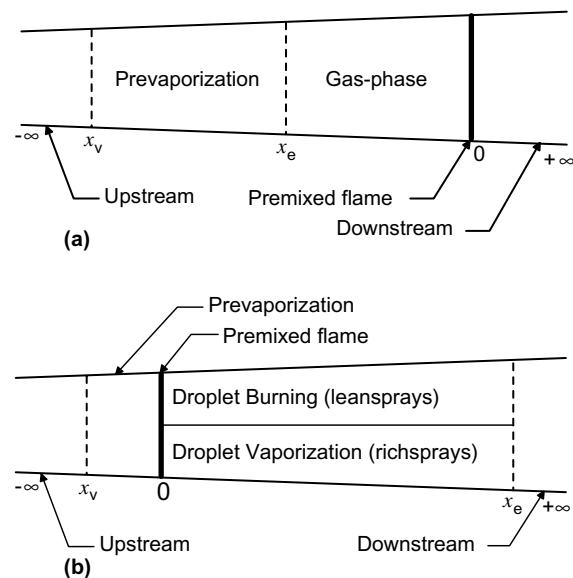


Fig. 1. Schematic diagram of: (a) completely prevaporized, and (b) partially prevaporized modes.

premixed flame is one-step overall, that the fuel droplets burn in the flame sheet limit, and that the conventional constant property simplifications apply. More detailed assumptions and comments were described in the earlier study [12].

2.2. Governing equations

The total number of droplets crossing any plane normal to the cross-section is constant and expressed as

$$n'u'A' = n'_{-\infty}u'_{-\infty}A'_{-\infty} \quad (1)$$

where n' is the number density and u' is the axial velocity. The overall continuity is given by

$$\rho'u'A' = \rho'_{-\infty}u'_{-\infty}A'_{-\infty} \quad (2)$$

where $\rho' = \rho'_G + \rho'_S$ is the density of the mixture, in which $\rho'_S = (4\pi/3)r'^3n'$ shows the spray density. The characteristic velocity for nondimensionalization is S_L^0 such that $u = u'/S_L^0$. Quantities with and without primes are dimensional and nondimensional, respectively.

We designate the extent of gas-phase heterogeneity by the parameter $Z = \rho'_G/\rho'$ such that $Z = 1$ represents the completely vaporized state. Following the previous formulation [12], the present case for a duct with varying cross-sectional area can be modeled by adding $-\rho Zu$, $(1/Le)(dY/dx)$, dT/dx times $(1/A)(dA/dx)$ [3] to the right-hand sides of the non-dimensional equations for gas-phase continuity, conservation of fuel, oxidizer, and energy to give

$$\begin{aligned} \frac{d}{dx}(\rho Zu) &= \frac{A_1}{ZT} (1 - Z_{-\infty})^{2/3} (1 - Z)^{1/3} F(T, Y_0) - (\rho Zu) \left(\frac{1}{A} \frac{dA}{dx} \right) \end{aligned} \quad (3)$$

$$\begin{aligned} \frac{d}{dx} \left(\rho Zu Y_F - \frac{1}{Le} \frac{dY_F}{dx} \right) &= \dot{W} + f_F \frac{d}{dx}(\rho Zu) + \frac{1}{Le} \frac{dY_F}{dx} \left(\frac{1}{A} \frac{dA}{dx} \right) \end{aligned} \quad (4)$$

$$\begin{aligned} \frac{d}{dx} \left(\rho Zu Y_O - \frac{1}{Le} \frac{dY_O}{dx} \right) &= \dot{W} + f_O \frac{d}{dx}(\rho Zu) + \frac{1}{Le} \frac{dY_O}{dx} \left(\frac{1}{A} \frac{dA}{dx} \right) \end{aligned} \quad (5)$$

$$\frac{d}{dx} \left(\rho Zu T - \frac{dT}{dx} \right) = -\dot{W} + f_T \frac{d}{dx}(\rho Zu) + \frac{dT}{dx} \left(\frac{1}{A} \frac{dA}{dx} \right) \quad (6)$$

where A is the cross-sectional area of the duct, and

$$A_1 = 3 \cdot \left(\frac{\lambda'}{r'_{-\infty} \dot{m}'_p} \right)^2 \left(\frac{P' \overline{M}'}{\overline{R} C'_{PG} Q'_C \rho'_L} \right) \quad (7)$$

$$\dot{W} = - \left(\frac{B'\sigma}{\tilde{M}_O} \right) \left(\frac{P'\tilde{M}'}{\tilde{R}} \right) \left(\frac{\lambda'}{C'_{PG}\dot{m}'_p} \right) Y_O Y_F \exp \left(- \frac{T_a}{T} \right) \quad (8)$$

note $x = x'/l'_T$ is the non-dimensional distance expressed in units of the preheat zone thickness, $l'_T = \lambda'/(C'_{PG}\dot{m}'_p)$, where λ' is the thermal conductivity, C'_{PG} the specific heat at constant pressure, and \dot{m}'_p the flame propagation flux of a homogeneous premixture. The function $A(x)$ denotes the cross-sectional area of the duct, which is chosen to be a slowly varying function of x . Accordingly, $(1/A)(dA/dx)$ is of $O(\varepsilon)$ in the asymptotic analysis. In the following derivation, $(1/A)(dA/dx)$ will be stretched as $\varepsilon\Gamma$ [8]. Here Γ is called the stretch parameter. A positive value of Γ means that the flame propagates in a divergent section, while a negative value of Γ denotes that the flame propagates in a convergent section. $h_{LG} = h'_{LG}/Q'_C$ represents the latent heat of vaporization for the liquid fuel, and Q'_C is the heat of combustion per unit mass of gaseous fuel.

For the present problem it is convenient to use an alternate density parameter [12]

$$\xi = \frac{1-Z}{1-Z_{-\infty}} \quad (9)$$

instead of Z . Thus in a dilute spray we can expand $Z_{-\infty} = 1 - \varepsilon\gamma$ such that $Z = 1 - \varepsilon\gamma\xi$. The liquid loading will be denoted by the parameter γ .

In Eqs. (3)–(6), the function $F(T, Y_O)$ and the constant parameters $f_F, f_O,$ and f_T are, respectively, $\ln[1 + (T - T_b)/h_{LG}]$, 1, 0 and $-h_{LG}$ for the vaporizing droplets and $\ln[1 + (T - T_b - Y_O)/h_{LG}]$, 0, 1, and $(1 - h_{LG})$ for the burning droplets. In this study, we assume $T_{-\infty} = T_u$ for simplification.

2.3. Outer expansion

In the broad outer zones, reaction is effectively suppressed because of the temperature-sensitive Arrhenius kinetics. Thus expanding ξ, Y_F, Y_O and T in terms of ε as

$$\begin{aligned} \xi_{out}^{\pm} &= \xi_0^{\pm} + \varepsilon\xi_1^{\pm} + O(\varepsilon^2) \\ (Y_F)_{out}^{\pm} &= Y_{F0}^{\pm} + \varepsilon Y_{F1}^{\pm} + O(\varepsilon^2) \\ (Y_O)_{out}^{\pm} &= Y_{O0}^{\pm} + \varepsilon Y_{O1}^{\pm} + O(\varepsilon^2) \\ T_{out}^{\pm} &= T_0^{\pm} + \varepsilon T_1^{\pm} + O(\varepsilon^2) \end{aligned} \quad (10)$$

Substituting them into Eqs. (3)–(6), and expanding, we have

$$\frac{d}{dx}(\rho_0 u_0) = \frac{d}{dx}(\dot{m}_0) = 0 \quad (11)$$

$$\dot{m}_0 \frac{d\xi_0^{\pm}}{dx} + \frac{A_1}{T_0^{\pm}} (\xi_0^{\pm})^{1/3} \ln \left[1 + \frac{(T_0^{\pm} - T_b)}{h_{LG}} \right] + O(\varepsilon^2) = 0 \quad (12)$$

$$\begin{aligned} &\left[\frac{d}{dx}(\dot{m}_0 Y_{F0}^{\pm}) - \frac{1}{Le} \frac{d^2 Y_{F0}^{\pm}}{dx^2} \right] \\ &+ \varepsilon \left[\frac{1}{Le} \frac{d^2 Y_{F1}^{\pm}}{dx^2} - \frac{d}{dx}(\dot{m}_0 Y_{F1}^{\pm} - \dot{m}_0 \xi_0^{\pm} \gamma Y_{F0}^{\pm}) + \frac{\Gamma}{Le} \frac{dY_{F0}^{\pm}}{dx} \right] \\ &+ O(\varepsilon^2) = 0 \end{aligned} \quad (13)$$

$$\begin{aligned} &\left[\frac{d}{dx}(\dot{m}_0 Y_{O0}^{\pm}) - \frac{1}{Le} \frac{d^2 Y_{O0}^{\pm}}{dx^2} \right] \\ &+ \varepsilon \left[\frac{1}{Le} \frac{d^2 Y_{O1}^{\pm}}{dx^2} - \frac{d}{dx}(\dot{m}_0 Y_{O1}^{\pm} - \dot{m}_0 \xi_0^{\pm} \gamma Y_{O0}^{\pm}) + \frac{\Gamma}{Le} \frac{dY_{O0}^{\pm}}{dx} \right] \\ &+ O(\varepsilon^2) = 0 \end{aligned} \quad (14)$$

$$\begin{aligned} &\left[\frac{d^2 T_0^{\pm}}{dx^2} - \frac{d}{dx}(\dot{m}_0 T_0^{\pm}) \right] \\ &+ \varepsilon \left[T_{\infty} \frac{d^2 T_1^{\pm}}{dx^2} - T_{\infty} \frac{d}{dx}(\dot{m}_0 T_1^{\pm}) + \frac{d}{dx}(\dot{m}_0 \gamma T_0^{\pm} \xi_0^{\pm}) \right. \\ &\left. + h_{LG} \frac{d}{dx}(\dot{m}_0 \gamma \xi_0^{\pm}) + \Gamma \frac{dT_0^{\pm}}{dx} \right] + O(\varepsilon^2) = 0 \end{aligned} \quad (15)$$

2.4. Inner expansion

In the inner zone of the bulk gas-phase flame, the solution is expanded around the flame-sheet limit as

$$\begin{aligned} \xi_{in} &= \xi_f + O(\varepsilon) \\ (Y_F)_{in} &= Y_{Ff} + \varepsilon\beta_F + O(\varepsilon^2) \\ (Y_O)_{in} &= Y_{Of} + \varepsilon\beta_O + O(\varepsilon^2) \\ T_{in} &= T_{\infty} + \varepsilon T_{\infty}\theta + O(\varepsilon^2) \end{aligned} \quad (16)$$

with the stretched inner variable being $\eta = x/\varepsilon$. By inserting the inner expansion Eq. (16) into Eqs. (3)–(6), then

$$\frac{d\xi_f}{d\eta} = 0 \quad (17)$$

$$\begin{aligned} \frac{1}{Le} \frac{d^2 \beta_F}{d\eta^2} &= \frac{1}{Le} \frac{d^2 \beta_O}{d\eta^2} = -T_{\infty} \frac{d^2 \theta}{d\eta^2} \\ &= \frac{A}{2} (Y_{Ff} + \varepsilon\beta_F)(Y_{Of} + \varepsilon\beta_O) \exp \theta \end{aligned} \quad (18)$$

where

$$A = 2 \left(\frac{T_{\infty}}{T_a} \right) \left(\frac{B'\sigma}{\tilde{M}'_O} \right) \left(\frac{P'\tilde{M}'}{\tilde{R}} \right)^2 \left(\frac{\lambda'}{C'_{PG}\dot{m}'_p} \right) \exp \left(- \frac{T_a}{T_{\infty}} \right) \quad (19)$$

is the flame speed eigenvalue.

2.5. Boundary and jump conditions

Eqs. (12)–(15), (17) and (18) are subjected to the following boundary and jump conditions:

$$x = -\infty : \xi = 1, Y_F = Y_{F-\infty}, Y_O = Y_{O-\infty}, T = T_{-\infty} \quad (20)$$

$$x = x_v : \xi = 1, \quad Y_{F1}^- = Y_{O1}^- = T_1^- = 0, \quad T = T_b \quad (21)$$

$$x = x_e \text{ (completely prevaporized spray): } \xi = 0 \quad (22)$$

$$x = 0 : \xi = \xi_f, \quad Y_{F0}^- = Y_{F0}^+, \quad Y_{O0}^- = Y_{O0}^+, \\ T_0^- = T_0^+, \quad Y_{F1}^- - Y_{F1}^+ = Y_{O1}^- - Y_{O1}^+ = T_1^- - T_1^+ \quad (23)$$

$$x = x_e \text{ (partially prevaporized spray): } \xi = 0 \\ Y_F = (1 - \alpha)(Y_{j\infty} + \varepsilon\gamma) \\ Y_O = \alpha(Y_{j\infty} - \varepsilon\gamma) \\ T = T_\infty + \varepsilon T_\infty T_{1\infty} \quad (24)$$

$$x = +\infty : \xi = 0, \quad Y_F = (1 - \alpha)(Y_{j\infty} + \varepsilon\gamma) \\ Y_O = \alpha(Y_{j\infty} - \varepsilon\gamma) \\ T = T_\infty + \varepsilon T_\infty T_{1\infty} \quad (25)$$

where, for compactness of notation, we shall use $\alpha = 1$, $i = F, j = O$ for lean flame and $\alpha = 0$, $i = O, j = F$ for rich flame. T_∞ and $T_{1\infty}$ can be determined through energy balance between the far upstream and downstream states, thus we have

$$T_\infty - T_{-\infty} = Y_{j-\infty} - Y_{j\infty} = Y_{i-\infty} \quad (26)$$

2.6. Zeroth-order solutions

The zeroth-order solutions can be readily solved to be

$$Y_{F0}^- = Y_{F-\infty} - Y_{i-\infty} e^{Le\dot{m}_0 x}, \quad Y_{F0}^+ = (1 - \alpha)Y_{j\infty} \\ Y_{O0}^- = Y_{O-\infty} - Y_{i-\infty} e^{Le\dot{m}_0 x}, \quad Y_{O0}^+ = \alpha Y_{j\infty} \\ T_0^- = T_{-\infty} + Y_{i-\infty} e^{\dot{m}_0 x}, \quad T_0^+ = T_\infty \quad (27)$$

which are exactly the solutions for the initially gas-phase mixture because of the dilute spray assumption. Therefore, the influences of liquid loading is manifested only in the first and higher order terms.

Using these relations, we find

$$x_v = \frac{1}{\dot{m}_0} \ln \left(\frac{T_b - T_{-\infty}}{T_\infty - T_{-\infty}} \right) \quad (28)$$

as well as ξ_0^\pm , ξ_f and x_e . That is, for the completely prevaporized mode, we have

$$(\xi_0^-)^{2/3} = 1 - \frac{2A_1}{3\dot{m}_0} \int_{x_v}^x (T_{-\infty} + Y_{i-\infty} e^{\dot{m}_0 x})^{-1} \\ \times \ln \left[1 + \frac{(T_{-\infty} - T_b) + Y_{i-\infty} e^{\dot{m}_0 x}}{h_{LG}} \right] dx \quad (29)$$

from which x_e is determined by evaluating Eq. (29) with $\xi_0^- = 0$ at $x = x_e$. For the partially prevaporized mode, ξ_0^- is still given by Eq. (29), while

$$(\xi_0^+)^{2/3} = \xi_f^{2/3} - \frac{2A_1}{3\dot{m}_0 T_\infty} \\ \times \ln \left(1 + \frac{T_\infty - T_b + \alpha Y_{j\infty}}{h_{LG}} \right) x \quad (30)$$

from which x_e is determined by evaluating Eq. (30) with $\xi_0^+ = 0$ at $x = x_e$, while ξ_f is determined by evaluating Eq. (29) with $\xi_0^+ = \xi_f$ at $x = 0$.

2.7. Final solutions

By using the local Shvab-Zeldovich formulation and the detailed matching conditions at $\eta \rightarrow \pm \infty$ [12] to match the inner and outer solutions, we obtain the final results as follows:

$$\dot{m}_0^2 = \exp[T_1^+(0)] \quad (31)$$

in which $T_1^+(0)$ denotes the first-order downstream temperature perturbation at the flame. Eq. (31) indicates that the flame propagation flux is exponentially affected by the first-order temperature downstream near the flame. Adding Eq. (4) to Eq. (6) and integrating from $x = -\infty$ to $x = 0^+$ yields

$$T_1^+(0) = \frac{\gamma}{T_\infty} \left[\alpha - h_{LG} + (T_b - T_\infty) - \frac{C'_{PL}}{C'_{PG}} (T_b - T_\infty) \right] \\ \times \left(\frac{\dot{m}_0 \gamma}{T_\infty} \right) (T_\infty + h_{LG} - \alpha) \int_0^{x_e} \xi_0^+ e^{-\dot{m}_0 u} du \\ - \frac{\Gamma Y_{i-\infty}}{\dot{m}_0 T_\infty} \left(1 - \frac{1}{Le} \right) \quad (32)$$

where

$$x_e = \xi_f^{2/3} \frac{3\dot{m}_0 T_\infty}{2A_1} \left[\ln \left(1 + \frac{T_\infty - T_b + \alpha Y_{j\infty}}{h_{LG}} \right) \right]^{-1} \quad (33)$$

The first and second terms on the right-hand side of Eq. (32) show the spray effect, including droplet size ($r'_{-\infty}$) and liquid-fuel loading (γ), while the third term shows the coupled effects of Lewis number (Le) and stretch (Γ).

For the sake of notation compactness, we use $\alpha = 1$ for lean sprays and $\alpha = 0$ for rich sprays. The liquid fuel loading is represented by γ through the expansion of $Z_{-\infty} = 1 - \varepsilon\gamma$ for dilute sprays [12].

For completely prevaporized sprays, the value of x_e is equal to zero, so we obtain

$$\dot{m}_0^2 = \exp[T_{1\infty}] \quad (34)$$

where

$$T_{1\infty} = \frac{\gamma}{T_\infty} \left[\alpha - h_{LG} + (T_b - T_\infty) - \frac{C'_{PL}}{C'_{PG}} (T_b - T_\infty) \right] \\ - \frac{\Gamma Y_{i-\infty}}{\dot{m}_0 T_\infty} \left(1 - \frac{1}{Le} \right) \quad (35)$$

Here we use $i = F$ for lean sprays and $i = O$ for rich sprays. Eq. (35) also indicates that in the completely prevaporized mode, the flame propagation flux is independent of the initial liquid droplet size.

Note that the last term in Eq. (32) or (35), $-\frac{\Gamma Y_{i-\infty}}{\dot{m}_0 T_\infty} (1 - \frac{1}{Le})$, shows the coupled effects of Lewis

number (Le) and stretch (Γ). The influence of stretch becomes especially pronounced in the presence of preferential diffusion, when the mixture has a non-unity Lewis number. The variation of \dot{m}_0 depends on the sign of Γ and whether Le is greater or less than one. When $Le = 1$ or $\Gamma = 0$, the last term in Eq. (32) or (35) vanishes and the coupled effects of stretch and preferential diffusion disappear. Accordingly, the combustion characteristics would be similar to those of the previous studies [9–12] in which premixed flames propagate in a duct with constant cross-sectional area. When $Le < 1$ and $\Gamma > 0$ (or $Le > 1$ and $\Gamma < 0$), the sign of the last term in Eq. (32) or (35), $-\frac{\Gamma Y_{i\infty}}{\dot{m}_0 T_{i\infty}}(1 - \frac{1}{Le})$, is positive, indicating that the combined effects of Lewis number (Le) and stretch (Γ) strengthens the burning intensity of spray flame.

3. Results and discussion

On the basis of the formulated results, Eqs. (31) and (34), sample calculations for methanol and ethanol burning in air are now considered in a nonconserved manner which maintains the initial gas-phase composition but varies the liquid fuel loading. The influence of flame stretch and preferential diffusion on dilute spray flames in the problem will be assessed based on four parameters, namely the initial droplet radius (r'_{∞}), the liquid fuel loading (γ), flow stretch (Γ), and Lewis number (Le). Here r'_{∞} and γ show the internal heat transfer (heat gain or heat loss) for the fuel spray. Γ denotes the stretch parameter. A positive value of Γ means that the flame propagates in a divergent duct, while a negative value of Γ denotes that the flame propagates in a convergent duct. Lewis number is defined as $\lambda' / (\rho'_G C'_{PG} D'_i)$ in which the diffusion coefficient of the deficient reactant in the mixture is used. The results of lean methanol-spray flames with $Le > 1$ and rich methanol-spray flames with $Le < 1$ (or rich ethanol-spray flames $Le > 1$) are separately discussed in the following sections.

3.1. Lean methanol-spray flame with $Le > 1$

Fig. 2 demonstrates the flame propagation flux (\dot{m}_0) as a function of Γ , γ and r'_{∞} for a lean methanol-spray flame of $\Phi_G = 0.8$ and $Le = 1.04$. In the figure, the words “flame intensifying” and “flame weakening” are written with arrows to show the effects on spray flame. Additionally, the dashed line and solid line represent the CPM and PPM, respectively.

We first discuss the effect of liquid fuel loading on flame characteristics of lean spray flames. Fig. 2 shows that for a positively-stretched flame ($\Gamma > 0$) with a given γ , the increase of Γ first leads to the decrease of \dot{m}_0 , indicating that a larger positive stretch weakens the burning intensity, and finally results in flame extinction when the

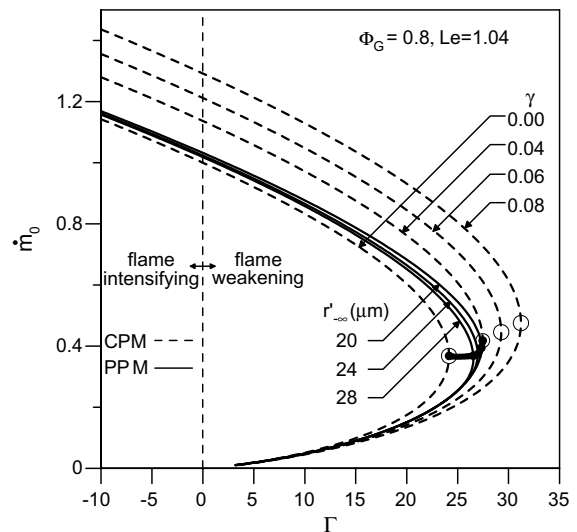


Fig. 2. Flame propagation flux (\dot{m}_0) as a function of the flame stretch (Γ) with various values of the liquid fuel loading (γ) and r'_{∞} for a lean methanol-spray flame.

flame stretch is large enough. This is mainly due to the suppression of burning intensity by positive stretch for a $Le > 1$ flame. Conversely, when the stretch is negative ($\Gamma < 0$), flame extinction does not occur with decreasing Γ because the negative stretch will strengthen the burning intensity. The upper and lower branches of the C-shaped extinction curves correspond to the stable and unstable solutions, respectively, and are connected at critical points represented by the symbol \circ . The critical points are identified as the occurrences of flame extinction. A lean spray containing a smaller amount of liquid loading has weaker prevaporization upstream of the flame, which provides a smaller amount of internal heat gain, and therefore has a weakened burning intensity. Accordingly, it can be extinguished by a smaller flame stretch.

Considering the partially prevaporized sprays ($r'_{\infty} > r'_c$), the influence of the initial droplet size on flame characteristics of a lean methanol-spray flame ($\Phi_G = 0.8$, $\gamma = 0.04$, and $Le = 1.04$) is shown by the solid lines in Fig. 2. It is seen that with increasing initial droplet size, the upper branch corresponding to the stable solution for a partially prevaporized spray deviates from that for the completely prevaporized spray ($r'_{\infty} \leq r'_c$), and approaches that for a homogeneous mixture ($\gamma = 0$). This feature indicates that for a $Le > 1$ flame under a positive stretch ($\Gamma > 0$), the flame propagation flux decreases as initial droplet size or flame stretch increases. The former is due to the reduction of internal heat gain; the latter is caused by the augmentation of the $Le > 1$ effect. Considering the droplet gasification process for a lean spray, the droplet absorbs heat for upstream vaporization, produces the secondary gasified fuel for

the bulk gas-phase burning, burns through droplet combustion afterwards, and finally results in a positive effect on $T_1^+(0)$. Therefore, the flame propagation flux of a lean spray decreases with decreasing liquid fuel loading or increasing initial droplet size.

The flame propagation flux at extinction, \dot{m}_E , as a function of Γ for various values of $r'_{-\infty}$ and γ in lean sprays is shown in Fig. 3. In the figure, the dashed lines denote constant- γ lines, while the solid lines denote constant- $r'_{-\infty}$ lines. Fig. 3 illustrates that \dot{m}_E and its corresponding flame stretch (Γ) at extinction increase with increasing γ or decreasing $r'_{-\infty}$. As described above, flame extinction characterized by a C-shaped curve for the lean-methanol spray flame with $Le > 1$ is governed by the positive flame stretch. It is known that a lean methanol-spray flame ($Le > 1$) containing a larger γ or a smaller droplet size has a higher burning intensity due to additional internal heat gain from burning secondary gasified fuel. Therefore, for a lean spray, it is expected that increasing γ or decreasing $r'_{-\infty}$ augments the secondary gasified fuel, resulting in the intensification of burning intensity, and consequently, the critical values of \dot{m}_E and its corresponding flame stretch at extinction increase.

3.2. Rich methanol-spray flames with $Le < 1$

The flame propagation flux \dot{m}_0 as a function of Γ and γ under completely prevaporized sprays for rich methanol-spray flames of $\Phi_G = 1.6$ and $Le = 0.94$ with small values of liquid fuel loading is shown on the left-hand side of Fig. 4. Contrary to the lean spray, the liquid fuel

absorbs heat for upstream prevaporization, producing the secondary gasified fuel which is equivalent to an inert substance without any contribution to burning for a rich spray. That is, the liquid fuel for rich sprays only absorbs heat for vaporization and thus provides an overall internal heat loss, eventually leading to the weakening of the burning intensity. Therefore, for a given Γ , the increase of γ leads to the decrease of \dot{m}_0 because a larger γ absorbs a larger amount of heat from flame for upstream droplets evaporation, which represents a larger amount of internal heat loss.

For a negatively-stretched flame ($\Gamma < 0$) with a given γ , the decrease of Γ leads to the decrease of \dot{m}_0 , and finally results in flame extinction characterized by a C-shaped curve. This is caused by the weakening effect of negative stretch for a $Le < 1$ flame. The extinction points are represented by the symbol \odot . However, when the $Le < 1$ flame experiences positive stretch ($\Gamma > 0$), the flame propagation flux increases with increasing flame stretch, and hence no extinction occurs.

Considering partially prevaporized sprays, the effects of flame stretch (Γ) and initial droplets size ($r'_{-\infty}$) on rich methanol-spray flames of $\Phi_G = 1.6$, $\gamma = 0.2$, and $Le = 0.94$ are shown in Fig. 4. It is seen that with increasing initial droplet size, the flame propagation flux deviates from that for the completely prevaporized spray ($r'_{-\infty} \leq r'_c$), and approaches that for a homogeneous mixture ($\gamma = 0$). This indicates that the flame propagation flux increases with increased initial droplet size or flame stretch. The former is due to the reduction of internal heat loss; the latter is caused by the enhancement of the $Le < 1$ effect. A rich spray containing larger

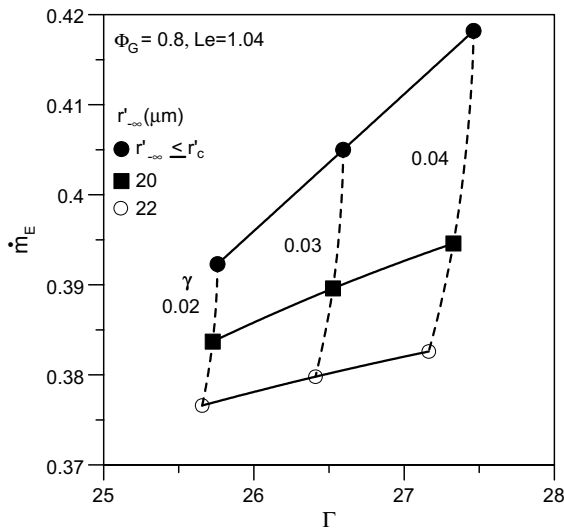


Fig. 3. The flame propagation flux at extinction \dot{m}_E as a function of the flame stretch (Γ) and the liquid fuel loading (γ) for a lean methanol-spray flame.

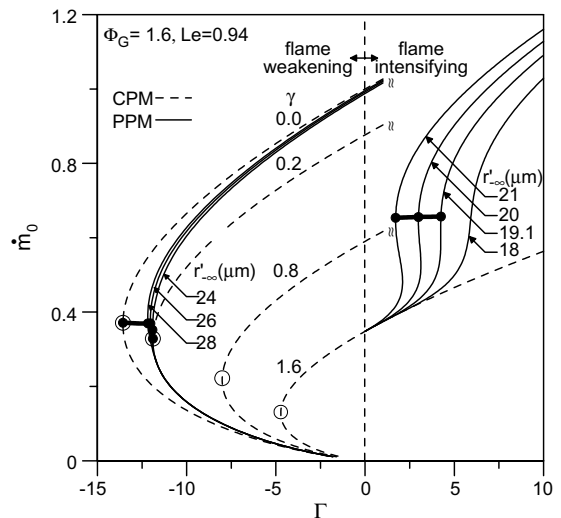


Fig. 4. Flame propagation flux (\dot{m}_0) as a function of the flame stretch (Γ) with various values of $r'_{-\infty}$ and liquid fuel loading (γ) for a rich methanol-spray flame.

droplets has a smaller prevaporization upstream corresponding to a lower internal heat loss, therefore, it has an enhanced burning intensity.

The variations of \dot{m}_0 with Γ and $r'_{-\infty}$ for the rich methanol-spray flame with a fixed amount of liquid loading ($\gamma = 1.6$) are shown on the right-hand side of Fig. 4. The results show that \dot{m}_0 increases with increasing flame stretch or initial droplet size. As explained above, the former is due to the enhancement of the $Le < 1$ effect; the latter is caused by the reduction of internal heat loss coming from droplets vaporization. For a given value of $r'_{-\infty}$ below a critical value (i.e., $r'_{-\infty} < r'_{-\infty}^* = 19.1 \mu\text{m}$), the characteristic curve of \dot{m}_0 shows that by decreasing the flame stretch from a large positive value, the flame propagation flux initially influenced by the partially prevaporized mode is monotonically reduced and eventually merges into the completely prevaporized mode at which $r'_{-\infty} = r'_{-\infty}^*$; therefore, flame extinction does not occur under the condition of PPM but rather CPM. However, if the droplet size is large enough (i.e., $r'_{-\infty} \geq r'_{-\infty}^* = 19.1 \mu\text{m}$), the flame enduring positive stretch can be extinguished, and an S-shaped extinction curve can occur. The extinction points are designated by the symbol \bullet . The S-shaped extinction curve (a triple-valued function), which differs from the C-shaped one (a double-valued function), demonstrates that the flame extinction is dominated by internal heat loss coming from droplet vaporization. This suggests that a spray having droplets large enough can considerably change the temperature gradients near the flame, resulting in flame extinction for a $Le < 1$ flame experiencing a small positive flame stretch. This characteristic was also found in our previous study [13] in which the occurrence of the S-shaped curve for spray flames in a stagnation-point flow was extensively discussed.

For rich methanol-spray flames, the flame propagation flux at extinction, \dot{m}_E , as a function of Γ for various values of $r'_{-\infty}$ and γ is shown in Fig. 5. When the liquid loading (γ) is small, e.g., $\gamma = 0.1, 0.15$ and 0.2 , only C-shaped extinction curves is present. Flame extinction characterized by a C-shaped curve for the rich-methanol spray flame ($Le < 1$) with a small γ is mainly controlled by the negative flame stretch. A rich spray containing a smaller amount of liquid fuel loading or larger droplets with weaker prevaporization upstream of the flame results in reduced internal heat loss and therefore an intensified burning intensity. In the lower half of Fig. 5, it is seen that \dot{m}_E is increased with increasing $r'_{-\infty}$ or decreasing γ due to the reduction of internal heat loss coming from droplet vaporization. Thereby, with increasing $r'_{-\infty}$ or decreasing γ , the value of Γ at extinction decreases, i.e., the negative stretch effect required for flame extinction increases.

However, when the liquid loading is thick enough, e.g., $\gamma = 1.6, 1.7$ and 1.8 in the upper half of Fig. 5, the S-shaped extinction curve occurs if the initial droplet

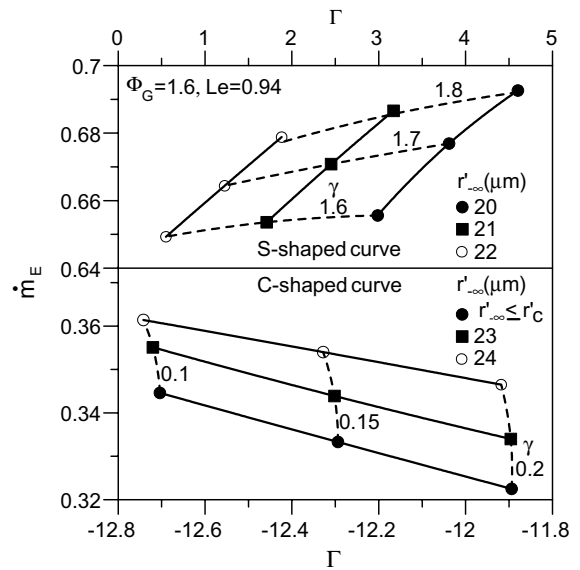


Fig. 5. The flame propagation flux at extinction \dot{m}_E as a function of the flame stretch (Γ) and the liquid fuel loading (γ) for a rich methanol-spray flame.

size is sufficiently large. The S-shaped extinction curve differs from the C-shaped one in the fact that, for a $Le < 1$ methanol-spray flame experiencing small positive stretch, the flame extinction is dominated by internal heat loss when the partially prevaporized spray is composed of sufficiently large liquid fuel loading and droplet size. For a given γ , both \dot{m}_E and its corresponding flame stretch at extinction increase with decreasing $r'_{-\infty}$. This characteristic is the same as what is illustrated on the right-hand side of Fig. 4. Furthermore, for a fixed value of $r'_{-\infty}$, the enlargement of liquid loading results in the increase of \dot{m}_E and its corresponding flame stretch required for extinction.

3.3. Rich ethanol-spray flames with $Le > 1$

Fig. 6 demonstrates the flame propagation flux (\dot{m}_0) as a function of Γ , γ and $r'_{-\infty}$ for a rich ethanol-spray flame of $\Phi_G = 1.5$ and $Le = 1.22$. We first discuss the results of completely prevaporized sprays ($r'_{-\infty} \leq r'_{-\infty}^*$) shown by the dashed lines. Note that for a positively-stretched flame ($\Gamma > 0$) with a given γ , the increase of Γ first leads to the decrease of \dot{m}_0 and finally results in flame extinction when the flame stretch is large enough. This characteristic results mainly from the suppression of burning intensity by positive stretch for a $Le > 1$ flame; and it is the same as in Fig. 2. On the contrary, when the stretch is negative ($\Gamma < 0$), flame extinction does not occur with decreasing Γ because the negative stretch will have strengthening-effect on the burning intensity. A rich spray containing a smaller amount of

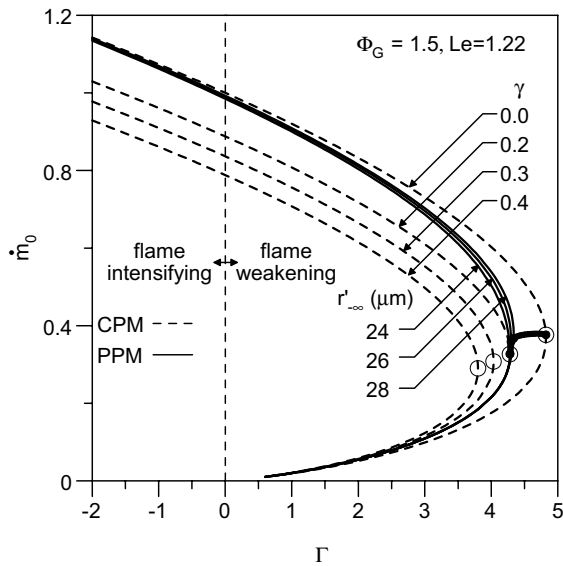


Fig. 6. Flame propagation flux (\dot{m}_0) as a function of the flame stretch (Γ) with various values of the liquid fuel loading (γ) and $r'_{-\infty}$ for a rich ethanol-spray flame.

liquid fuel loading absorbs less heat for droplet vaporization upstream of the flame and thus the flame suffers a smaller amount of internal heat loss. Accordingly, a premixed flame with $Le > 1$ under the influence of a smaller γ will be extinguished by a larger positive stretch effect, i.e. a larger value of Γ .

Considering the partially prevaporized sprays ($r'_{-\infty} > r'_c$), the influence of the initial droplet size on flame characteristics for rich ethanol-spray flame of $\Phi_G = 1.5$, $\gamma = 0.2$, and $Le = 1.22$ is shown in Fig. 6. With increasing initial droplet size, the upper branch corresponding to the stable solution for a partially prevaporized mode deviates from that for the completely prevaporized mode ($r'_{-\infty} \leq r'_c$), and approaches that for a homogeneous mixture ($\gamma = 0$). In other words, the flame propagation flux increases with increased initial droplet size, due to the reduction of internal heat loss. For a fixed amount of liquid loading γ , a larger droplet radius means less evaporation surface and thus less internal heat loss to act against the gaseous fuel burning. Therefore, for a given γ , the burning intensity of a premixed flame increases with increasing initial droplet size, leading to the occurrence of extinction at a larger positive stretch effect, i.e. a larger positive value of Γ .

For a rich ethanol-spray flame, the flame propagation flux at extinction, \dot{m}_E , as a function of Γ for various values of $r'_{-\infty}$ and γ is shown in Fig. 7. Flame extinction characterized by a C-shaped curve for the rich-ethanol spray flame with $Le > 1$ is dominated by the positive flame stretch. Reducing liquid fuel loading or increasing

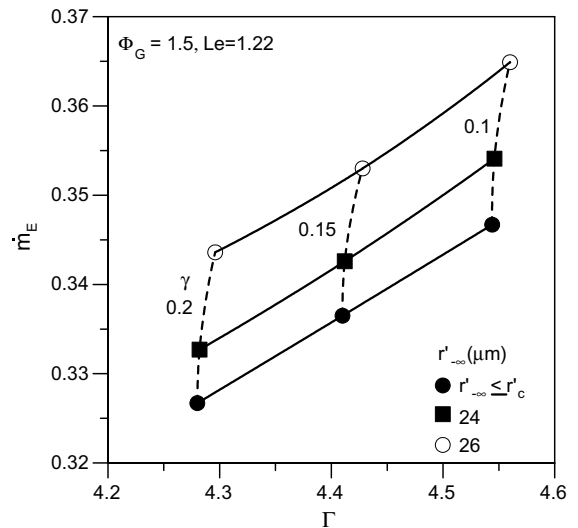


Fig. 7. The flame propagation flux at extinction \dot{m}_E as a function of the flame stretch (Γ) and the liquid fuel loading (γ) for a rich ethanol-spray flame.

droplet size in a rich spray leads to weaker prevaporization upstream of the flame so as to reduce internal heat loss and therefore elevate burning intensity. Accordingly, it is seen that \dot{m}_E and its corresponding flame stretch (Γ) at extinction is increased with increasing $r'_{-\infty}$ or decreasing γ because of the reduction in the heat loss due to droplet vaporization. That is, the positive stretch effect required for flame extinction characterized by a C-shape curve increases when the rich-ethanol spray contains a smaller liquid fuel loading or larger droplets.

4. Conclusions

Following activation energy asymptotics, an extinction theory of stretch premixed flames with combustible sprays was developed to explore the influence of liquid fuel spray, flame stretch, and Lewis number on the burning and extinction of both methanol and ethanol sprays. Results are summarized as follows:

1. The positive (or negative) stretch weakens and strengthens the burning intensity of a $Le > 1$ (or $Le < 1$) flame and a $Le < 1$ (or $Le > 1$) flame, respectively.
2. The internal heat transfer, which is associated with the liquid fuel loading and the initial droplet size of the spray, provides internal heat loss for rich sprays but heat gain for lean sprays. Therefore, for the spray flame with $Le > 1$, the burning intensity weakened by

the positive flame stretch can be enhanced (reduced) when the lean (rich) spray has a larger amount of liquid fuel loading or a smaller initial droplet size.

3. For a rich methanol-spray flame with $Le < 1$ enduring positive stretch, extinction does not occur for the completely prevaporized mode. However, an S-shaped extinction curve (a triple-valued function), which differs from the C-shaped one (a double-valued function), can occur if the liquid fuel loading is large enough and the droplet size is sufficiently large for the partially prevaporized mode.
4. Extinction characterized by a C-shaped curve is dominated by flame stretch; while extinction characterized by an S-shaped curve is governed by internal heat loss.

Acknowledgement

This work was partly supported by the National Science Council, Taiwan, ROC, under contract NSC91-E-168-006-014. Valuable comments by the reviewers of this report are kindly appreciated.

References

- [1] I. Ishizuka, C.K. Law, An experimental study on extinction and stability of stretch premixed flames, *Proc. Combust. Inst.* 19 (1982) 327–335.
- [2] Y.D. Kim, M. Matalon, Propagation and extinction of a premixed flame in a stagnation-point flow, *Combust. Flame* 73 (1988) 303–313.
- [3] J.D. Buckmaster, G.S.S. Ludford, *Theory of Laminar Flame*, Cambridge University Press, Cambridge, UK, 1982.
- [4] J. Sato, Effects of Lewis number on extinction behavior of premixed flames in a stagnation flow, *Proc. Combust. Inst.* 19 (1982) 1541–1548.
- [5] G.I. Sivashinsky, Structure of Bunsen flames, *J. Chem. Phys.* 62 (2) (1975) 638–643.
- [6] C.J. Sung, K.M. Yu, C.K. Law, On the geometry and burning intensity of Bunsen flames, *Combust. Sci. Technol.* 100 (1994) 245–270.
- [7] J. Buckmaster, A. Nachman, Propagation of an unsteady flame in a duct of varying cross-section, *Quart J Mech Appl Math* 34 (1981) 501–520.
- [8] J.H. Tien, Effects of flame stretch on premixed flame propagation in a closed tube, *Combust. Flame* 107 (1996) 303–306.
- [9] C.C. Liu, T.H. Lin, The interaction between external and internal heat loss on the flame extinction of dilute sprays, *Combust. Flame* 85 (1991) 468–478.
- [10] S.S. Hou, C.C. Liu, T.H. Lin, The influence of external heat transfer on flame extinction of dilute sprays, *Int. J. Heat Mass Transfer* 36 (7) (1993) 1867–1874.
- [11] S.S. Hou, T.H. Lin, A theory on excess enthalpy spray flame, *Atomizat Sprays* 9 (1999) 355–369.
- [12] T.H. Lin, C.K. Law, S.H. Chung, Theory of laminar flame propagation in off-stoichiometric dilute sprays, *Int. J. Heat Mass Transfer* 31 (5) (1988) 1023–1034.
- [13] S.S. Hou, T.H. Lin, Effects of internal heat transfer and preferential diffusion on stretched spray flames, *Int. J. Heat Mass Transfer* 44 (2001) 4391–4400.